

BPC 01270

Electrical excitability of artificial enzyme membranes

IV. Theoretical approach of the membrane potential of synthetic proteinic films

Alain Trubuil^b, Alain Friboulet^a, Rajani Joshi^b, Jean-Pierre Kernevez^b
and Daniel Thomas^a

^a *Laboratoire de Technologie Enzymatique, UA 523 du CNRS and* ^b *Département de Mathématiques Appliquées et d'Informatique, Université de Technologie de Compiègne, BP 649, 60206 Compiègne Cedex, France*

Received 5 January 1988

Accepted 7 April 1988

Membrane potential; Donnan layer; Artificial membrane

This paper deals with the theoretical approach of the membrane potential of artificial proteinic film. Programming techniques using finite difference simulations for the steady state and transient solutions of the Nernst-Planck and Poisson equations were used and solved by the collocation and corrector methods. This approach allows one to calculate the membrane potential without any discontinuity between the Donnan and the diffusion potentials, the thickness of the boundary layers being automatically determined by the intrinsic properties of the solution and of the membrane. The theoretical results are compared with experimental potentials measured on proteinic artificial films.

1. Introduction

A number of complex situations in biology and biophysics involve the interaction of electrolyte liquids with electrically charged bodies. The phenomena of ion transport and the flow of electrically charged fluids through the cell membrane, as the diffusion of ionic substrates and activators or inhibitors towards an enzyme which is bound to or embedded in a charged structure, represent such situations. The use of immobilized enzymes as a basis for the study of the enzymatic diffusion-reaction properties, especially concerning the phenomena of oscillations [1,2], hysteresis

[3,4] and wave propagation [5], as well as active transport models [6], allows the treatment of the electrolytic migration and diffusive effects. The artificial membrane systems of our interest consist of a proteinic film which offers amphoteric sites with weakly ionizable groups in which an enzyme can be homogeneously distributed. In equilibrium with an external solution, the distribution of the ionic species between the solutions and the charged matrix is governed by a Donnan equilibrium operating at the interface between the phases [7]. Nevertheless, the Donnan membrane theory, applied to fixed-charge membranes by Teorell [8], is essentially obtained from the equilibrium of the electrochemical potentials of ions at the membrane boundaries when the diffusion of ions inside the membrane is at steady state. The possibilities of departure from local equilibrium have been indicated at the interfaces of polymeric ion-exchange membranes [9].

Correspondence address: A. Friboulet, Laboratoire de Technologie Enzymatique, UA 523 du CNRS, Université de Technologie de Compiègne, BP 649, 60206 Compiègne Cedex, France.

Programming techniques using finite difference simulation for the steady state and transient solution of the Nernst-Planck and Poisson equation system have been previously described [10,11]. However, these techniques assume an a priori thickness of the boundary layer and use finite differences on an arbitrary number of spaced grid points. The method we test, collocation with an adaptive mesh, overcomes this difficulty since the program automatically adjusts the mesh to the nature of the solution. The usefulness of such a procedure is evident with systems in which a reaction can modify the ion-exchange properties within the thickness of the membrane and is well known to those dealing with non-linear problems where the solution involves sharp fronts.

2. Experimental procedure

2.1. Preparation of proteinic films

The proteinic films were produced according to a previously described cross-linking method [12]. The reaction was carried out for a period of 2 h with a solution containing 40 mg ml⁻¹ bovine serum albumin (Sigma, fraction V) and 4 mg ml⁻¹ glutaraldehyde in 20 mM sodium phosphate buffer at pH 6.8. The solution was spread onto a plane glass surface. After drying in a current of air, a 40 cm², 50 μm thick film was obtained.

2.2. Measurement of potential difference

The membrane was set in a diffusion cell where it separates two 25-ml compartments. The diffusion surface area was 0.5 cm². Both solutions were mixed and the concentrations were maintained constant with respect to time by means of a continuous flow of the solutions. The pH values were regulated on each side of the cell by a pH-stat apparatus and the solutions were thermostatted at 20°C. The membrane potential was permanently measured by means of two calomel reference electrodes with a vibrating-reed electrometer (Cary 401).

3. Mathematical formulation

When a membrane with fixed charges separates two compartments containing electrolyte solutions of monovalent ions (I⁺, I⁻), these ions move by diffusion-migration through the membrane, creating an electric field within it. The determination of the electrical potential, concentrations and flux of electrolyte liquids could be formulated to require the solutions of fluid dynamical equations for the liquid convection velocity v simultaneously with the classical Nernst-Planck flux equations and the flux continuity equation. With the assumption that the liquids flowing through the membrane are convectionless ($v = 0$), the above system would be defined mathematically by the following equations:

the flux:

$$\begin{cases} J_{I^+} = -D_{I^+}[(\partial[I^+]/\partial X) + \lambda[I^+](\partial\psi/\partial X)] \\ J_{I^-} = -D_{I^-}[(\partial[I^-]/\partial X) - \lambda[I^-](\partial\psi/\partial X)] \end{cases} \quad (1)$$

the mass-balance equation:

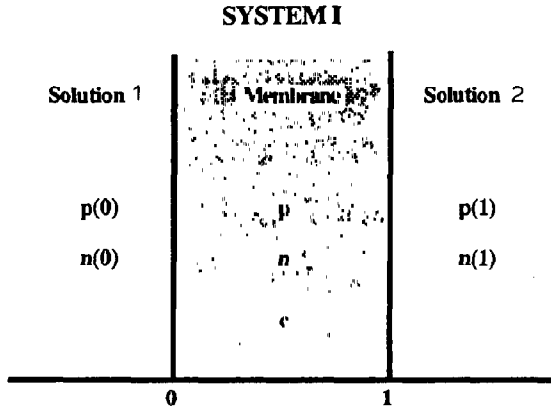
$$\begin{cases} (\partial[I^+]/\partial t) + (\partial J_{I^+}/\partial X) = 0 \\ (\partial[I^-]/\partial t) + (\partial J_{I^-}/\partial X) = 0; 0 < X < L; t > 0 \end{cases} \quad (2)$$

and the Poisson equation:

$$-[\epsilon](\partial^2\psi/\partial X^2) = [I^+] - [I^-] \pm [C^\pm] \quad (3)$$

where D_{I^+} and D_{I^-} represent the diffusion coefficients of the positive and negative ions, respectively; ψ , the potential of the electric field; $\lambda = F/RT$ (F , Faraday's constant; R , gas constant; T , absolute temperature); $[\epsilon] = D\epsilon_0/F$ (D , dielectric constant of the electrolyte liquid; ϵ_0 , permittivity of a vacuum), t , time; L , thickness of the one-dimensional membrane; and $[C^\pm]$, concentration of the fixed monovalent charges in the membrane.

We express these equations in dimensionless form by setting $p = [I^+]/K$; $n = [I^-]/K$; $c = [C^\pm]/K$; $\epsilon = [\epsilon]/KL^2$; $x = X/L$, etc., where K is a concentration (usually equal to $[I^+]_{(x=0)}$ and $D_p = D_{I^+}/d$; $D_n = D_{I^-}/d$ where d is usually D_{I^+} .



Scheme 1

The equations governing the system in the stationary state are then:

$$\left. \begin{aligned} dJ_p/dx &= 0 \\ J_p &= -D_p[(dp/dx) + \lambda p(dV/dx)] \\ dJ_n/dx &= 0 \\ J_n &= -D_n[(dn/dx) - \lambda n(dV/dx)] \\ -\epsilon(d^2V/dx^2) &= p - n \pm c; 0 < x < 1 \end{aligned} \right\} \quad (4)$$

with the boundary conditions:

$$\left. \begin{aligned} p_{(x=0)} &= p(0) = n(0) = \alpha > 0 \\ p_{(x=1)} &= p(1) = n(1) = \beta \geq \alpha; \alpha, \beta \text{ given} \\ \text{and } V(0) &= 0 \end{aligned} \right\} \quad (5)$$

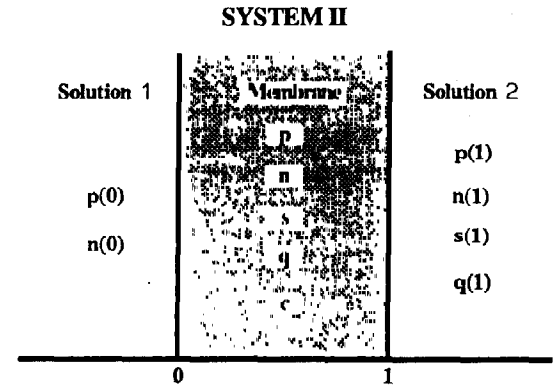
3.1. System 1

In this system (scheme 1), the membrane possesses monovalent, negative, fixed sites and V satisfies the condition of zero current ($J_p = J_n$). The system is governed by eqs. 4 and 5, with f given and $V(1)$ satisfying the following relation:

$$\left. \begin{aligned} J_p(1) &= J_n(1) \\ D_p[(dp(1)/dx) + \lambda p(1)(dV(1)/dx)] \\ &= D_n[(dn(1)/dx) - \lambda n(1)(dV(1)/dx)] \end{aligned} \right\} \quad (6)$$

3.2. System 2

Membrane system 1 is modified by the addition of a positively charged ion S^+ and its counterpart,



Scheme 2

negatively charged monovalent ion S^- in the electrolyte solution of compartment 1 (scheme 2). Representing by s and q the dimensionless forms of $[S^+]$ and $[S^-]$, respectively, the following set of equations define the system:

$$\left. \begin{aligned} dJ_s/dx &= 0 \\ J_s &= -D_s[(ds/dx) + \lambda s(dV/dx)] \\ dJ_p/dx &= 0 \\ J_p &= -D_p[(dp/dx) + \lambda p(dV/dx)] \\ dJ_q/dx &= 0 \\ J_q &= -D_q[(dq/dx) - \lambda q(dV/dx)] \\ dJ_n/dx &= 0 \\ J_n &= -D_n[(dn/dx) - \lambda n(dV/dx)] \end{aligned} \right\} \quad (7)$$

with the condition of zero current:

$$J_p + J_s = J_n + J_q$$

and the Poisson equation:

$$-\epsilon(d^2V/dx^2) = p + s - n - q - c$$

with the boundary conditions:

$$\left\{ \begin{aligned} p(0) &= n(0) = \alpha, \quad p(1) = n(1) = \beta \\ s(0) &= q(0) = 0, \quad s(1) = q(1) = \mu \\ V(0) &= 0 \end{aligned} \right\} \quad (8)$$

and $V(1)$ satisfies the condition of zero current:

$$J_p(1) + J_s(1) = J_n(1) + J_q(1)$$

4. Theoretical results

The main theoretical results for this singularly perturbed boundary value problem and particularly the existence theorem and asymptotic expansions were proved in the work of Henri and Louro [13].

4.1 Result 1

$(s_\epsilon, p_\epsilon, n_\epsilon, q_\epsilon, V_\epsilon)$ does not tend uniformly to (s, p, n, q, V) as ϵ tends to zero. (s, p, n, q, V) does not satisfy the boundary conditions. To determine a uniformly good approximation of $(s_\epsilon, p_\epsilon, n_\epsilon, q_\epsilon, V_\epsilon)$, we search a convector ϕ_ϵ so that $V_\epsilon - (V + \phi_\epsilon)$ tends to zero uniformly in the interval $[0, 1]$.

4.2. Result 2

$$\begin{aligned} s \exp(-\phi_\epsilon) - s_\epsilon &\rightarrow 0 && \text{uniformly over } [0,1] \\ p \exp(-\phi_\epsilon) - p_\epsilon &\rightarrow 0 && \text{uniformly over } [0,1] \\ n \exp(-\phi_\epsilon) - n_\epsilon &\rightarrow 0 && \text{uniformly over } [0,1] \\ q \exp(-\phi_\epsilon) - q_\epsilon &\rightarrow 0 && \text{uniformly over } [0,1] \\ V_\epsilon - (V + \phi_\epsilon) &\rightarrow 0 && \text{uniformly over } [0,1]. \end{aligned}$$

where (s, p, n, q, V) is the solution of the following problem in which the parameter ϵ has disappeared:

$$\left. \begin{aligned} -d^2s/dx^2 - d/dx(sdV/dx) &= 0 \\ -d^2p/dx^2 - d/dx(pdV/dx) &= 0 \\ -d^2n/dx^2 - d/dx(ndV/dx) &= 0 \\ -d^2q/dx^2 - d/dx(qdV/dx) &= 0 \\ p + s - n - q - f &= 0 \text{ electroneutrality} \\ dV/dx &= d/dx[(D_n n + D_q q - D_s s - D_p p)/ \\ &\quad (D_s s + D_p p + D_n n + D_q q)] \end{aligned} \right\} \quad (9)$$

with the boundary conditions:

$$\begin{aligned} s(0) &= (s_0/(s_0 + p_0)) \left(c/2 + ((c/2)^2 \right. \\ &\quad \left. + (so + po)(no + qo))^{1/2} \right) \end{aligned} \quad (10)$$

$$\begin{aligned} p(0) &= (p_0/(s_0 + p_0)) \left(c/2 + ((c/2)^2 \right. \\ &\quad \left. + (so + po)(no + qo))^{1/2} \right) \end{aligned} \quad (11)$$

$$\begin{aligned} n(0) &= (n_0/(s_0 + p_0)) \left(-c/2 + ((c/2)^2 \right. \\ &\quad \left. + (so + po)(no + qo))^{1/2} \right) \end{aligned} \quad (12)$$

$$\begin{aligned} q(0) &= (q_0/(s_0 + p_0)) \left(-c/2 + ((c/2)^2 \right. \\ &\quad \left. + (so + po)(no + qo))^{1/2} \right) \end{aligned} \quad (13)$$

$$\begin{aligned} V(0) &= -\log \left(\left\{ c/2 + ((c/2)^2 + (so + po) \right. \right. \\ &\quad \left. \left. \times (no + qo))^{1/2} \right\} \{ so + po \}^{-1} \right) \end{aligned} \quad (14)$$

The boundary conditions in extremity 1 are obtained by substitution of 1 for 0, and the corrector is characterized by the following equations:

$$\begin{aligned} \phi_\epsilon &= \phi_\epsilon^0 + \phi_\epsilon^1 \\ \text{with } \phi_\epsilon^0 &\text{ solution of:} \\ -\epsilon(d^2\phi_\epsilon^0/dx^2) &= [s(0) + p(0)] \\ &\quad \times \exp(-\phi_\epsilon^0) - [n(0) + q(0)] \\ &\quad \times \exp(\phi_\epsilon^0) - c \\ \phi_\epsilon^0(0) &= -V(0) = \ln \left(\left\{ c/2 + ((c/2)^2 \right. \right. \\ &\quad \left. \left. + (so + po)(no + qo))^{1/2} \right\} \{ so + po \}^{-1} \right) \\ \phi_\epsilon^0(1) &= 0 \end{aligned} \quad (15)$$

and ϕ_ϵ^1 solution of a similar equation.

5. Results

5.1. Numerical resolution

5.1.1. Collocation method (COLSYS [14])

For numerical solution of the two-point boundary problem, we use collocation at Gaussian points. This method can be formulated as a system of nonlinear differential equations which has to be solved numerically by an iterative method starting from an initial guess for the solution. The boundary layers in the neighbourhood of 0 and 1

lead to a very fine discretization and consequently high calculation time. So a more rapid method using the asymptotic expansions described above has been used.

5.1.2. Corrector method

The method consists in solving eqs. 9 with the boundary conditions, eqs. 10–14. We use COLSYS for the resolution, but with a coarse grid. On the other hand, we solve eq. 15 and the corresponding problem for ϕ_e^1 . The scale of the equations was changed and the problem was solved in the new system of coordinates. Finally, combination of the solutions for both problems gives the numerical result for the problem of diffusion. The results obtained with this method are very close to those of the collocation method; the approximation can be considered as realistic.

5.2. Outcome of numerical calculations and confrontation with experimental results

Proteinic artificial films offer amphoteric sites with weakly ionizable groups which give rise to

ion-exchange properties, which are functions of electrolyte concentration and pH [7]. Albumin membranes behave as cation-exchange matrices for pH values above 5. When such a membrane separates two compartments containing electrolyte solutions (I^+ , I^-), a potential difference can be experimentally measured.

5.2.1. System 1

By assuming a membrane thickness of 50 μm and diffusion coefficients $D_p = 1$ and $D_n = 0.766$, with a constant concentration difference between the two compartments ($p(0) = n(0) = 1$; $p(1) = n(1) = 10$), theoretical values of the potential difference can be obtained. The numerical method used in the calculation allows the determination of the profiles of the different ionic species and of the potential inside the membrane without any discontinuity between the Donnan layers and the membrane thickness. Fig. 1 shows the calculated profiles for different negative fixed-charge values of the artificial film. Intramembranal concentrations and potential are plotted as a function of $-\log(x)$ for $0 < x \leq 0.5$ and of $-\log(x-1)$ for $0.5 \leq x < 1$ to visualize the data in the Donnan

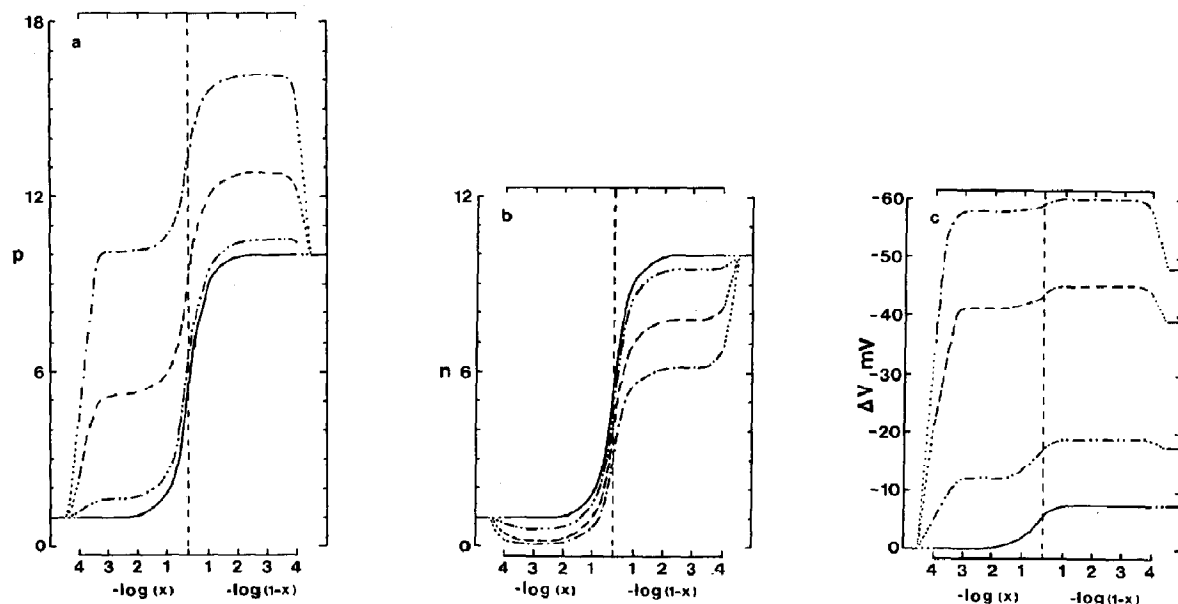


Fig. 1. System 1. Calculated intramembranal concentrations of I^+ (a), I^- (b) and electrical potential (c) as a function of $-\log(x)$ for $0 < x \leq 0.5$ and $-\log(1-x)$ for $0.5 \leq x < 1$, for different values of the fixed-charge density. $\alpha = 1$, $\beta = 10$, $D_p = 1$, $D_n = 0.766$. $c = 0$ (—), -1 (····), -5 (---) and -10 (----).

Table 1

Experimental and theoretical potential differences obtained with bovine serum albumin films

S.E., standard error of the mean. The number of independent experiments is indicated in parentheses. $\beta = 1$; $c = -6$; $D_p = 1$; $D_n = 0.766$.

α	Experimental ΔV (mV) (\pm S.E.)	Calculated potential (mV)
2.5	-20.25 ± 2.05 (4)	-20.69
5	-32.20 ± 1.85 (5)	-33.09
7.5	-38.70 ± 2.57 (5)	-38.58
10	-42.00 ± 2.42 (5)	-41.74

layers. The thickness of the layers where the Donnan potentials occur are always less than $x = 1 \times 10^{-3}$ (corresponding to 500 Å).

The experimental potential differences obtained when two solutions of $\text{Na}^+\text{H}_2\text{PO}_4^-$ are separated by an albumin membrane are shown in table 1. By assuming that the membrane bears a negative fixed-charge density $c = -6$, theoretical values were obtained (table 1). The two sets of values are in good agreement with each other. The determination of the profiles of the different ionic species and of the potential inside the membrane, including the Donnan layers, is depicted in fig. 2. In all cases, these results agree with the Donnan

Table 2

Experimental and theoretical potential differences obtained with system 2

S.E., standard error of the mean. The number of independent experiments is indicated in parentheses. $s(0) = q(0) = 0$; $p(0) = n(0) = p(1) = n(1) = 1$; $c = -6$. $D_p = 1$, $D_n = 0.766$, $D_s = 0.478$, $D_q = 0.681$.

$s(1) = q(1)$	Experimental ΔV (mV) (\pm S.E.)	Calculated ΔV (mV)
2.5	-15.75 ± 0.44 (4)	-16.01
5	-21.75 ± 0.59 (6)	-21.97
10	-26.20 ± 0.58 (6)	-26.49
20	-29.00 ± 0.92 (5)	-28.88
30	-29.90 ± 1.07 (6)	-29.25
40	-29.40 ± 1.23 (6)	-29.20
60	-28.15 ± 1.06 (5)	-28.70

exclusion theory; the lower the external concentration, the greater the Donnan exclusion.

5.2.2. System 2

We have previously shown [7] that when a proteinic membrane separates two compartments containing equal concentrations of sodium phosphate buffer, a potential difference can be measured when a salt (S^+ ; e.g., acetylcholine chloride) is injected into one compartment only. By assuming that $p(0) = p(1) = 1$, $n(0) = n(1) = 1$, $s(0) =$

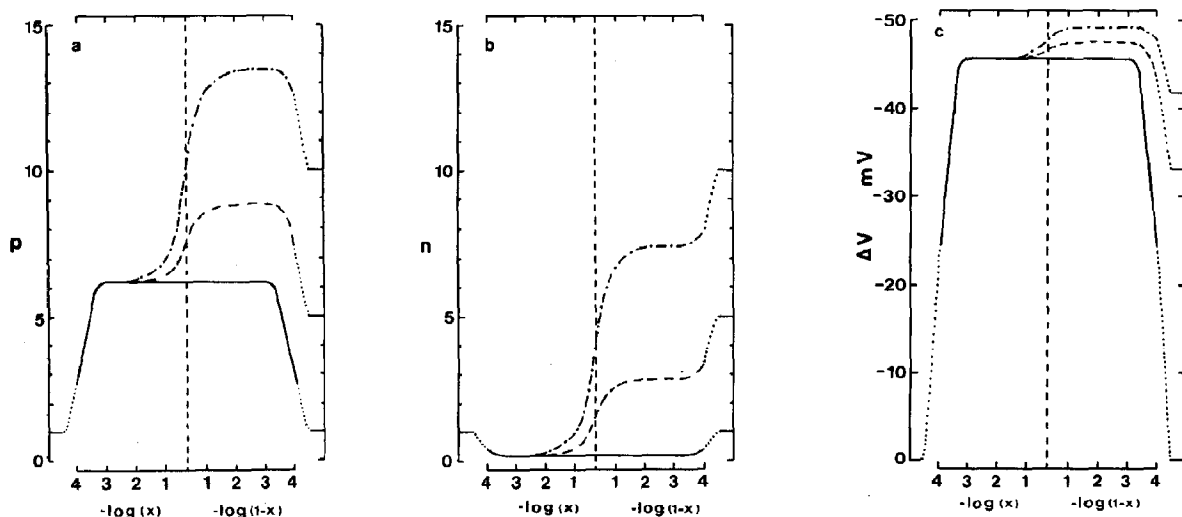


Fig. 2. System 1. Calculated ionic species and potential profiles plotted as fig. 1 for different ionic concentrations in compartment 1 for a defined fixed-charge density. $\alpha = 1$, $c = -6$, $D_p = 1$, $D_n = 0.766$. $\beta = 1$ (—), 5 (---) and 10 (·····).

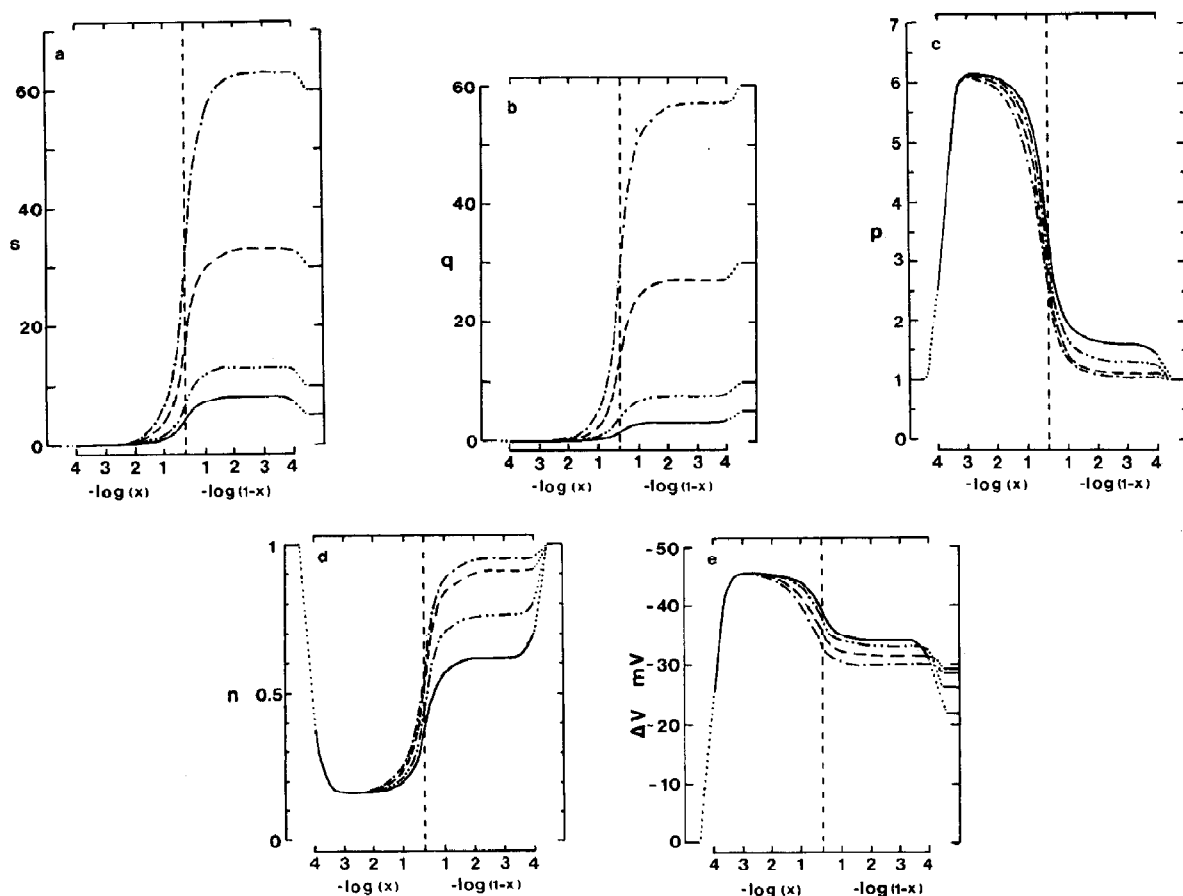


Fig. 3. Representation of the calculated profiles for different values of $s(1)$. $s(0) = q(0) = 0$; $c = -6$; $p(0) = n(0) = 1$; $p(1) = n(1) = 1$; $D_p = 1$; $D_n = 0.766$; $D_s = 0.478$; $D_q = 0.681$. $s(1) = 5$ (—), 10 (---), 30 (- - -) and 60 (· · · ·).

$q(0) = 0$, $c = -6$ and $D_p = 1$, $D_n = 0.766$, $D_s = 0.478$ and $D_q = 0.681$ (corresponding to the ratio of the diffusion coefficients in water), theoretical profiles of each of the components were obtained (fig. 3). The total potential obtained from these forms of ionic repartitioning are in good agreement with the experimental results (table 2).

6. Discussion

Knowledge of the repartitioning of the ionic concentrations and of the potential inside a structure is of great importance, since an enzyme activity present in a cellular compartment or immobilized in an artificial system can depend on the

local ionic concentrations and on the spatial repartitioning of a ionic substrate or effector. To determine these concentrations, one needs to calculate the Donnan and diffusion potentials in the system at the steady state or in evolution. Recently, Ohshima and Ohki [15] described a model for the potential distribution across a charged membrane, in which the membrane fixed charges are uniformly distributed through a layer of finite thickness at the membrane surface to account for the Donnan potential. They demonstrated that the apparent difference between the two concepts of the Donnan potential and the surface potential (or Gouy-Chapman double-layer potential) is not of a fundamental nature. However, in all cases the Donnan potential is calcu-

lated separately from the diffusion potential, for a layer of determined thickness. The aim of our present work was to test a method in which there is no fundamental distinction between the Donnan and diffusion potentials, without any prerequisite hypothesis about the thickness of the Donnan layer. The numerical methods used in this work allow one to solve such a problem of diffusion in electrically charged membranes when the fixed charges are kept constant, under both symmetrical and asymmetrical conditions. We obtain a very good agreement between the experimental data and the calculated results.

We have previously shown [2] that when an enzyme (e.g., acetylcholinesterase) able to induce local modifications of the fixed-charge concentration is immobilized in our artificial membranes, sophisticated forms of behavior such as hysteresis and oscillations of the membrane potential can be recorded. The next step of this work will be the generalization of our numerical method to simulate the membrane potential when the enzyme reaction modifies nonuniformly the density and/or the sign of the fixed charges and to devise a model of the nonlinear phenomena observed with the experimental system.

References

- 1 A. Naparstek, D. Thomas and S.R. Caplan, *Biochim. Biophys. Acta* 323 (1973) 643.
- 2 A. Friboulet and D. Thomas, *Biophys. Chem.* 16 (1982) 153.
- 3 A. Naparstek, J.L. Romette, J.P. Kernevez and D. Thomas, *Nature* 249 (1974) 490.
- 4 D. Thomas, J.N. Barbotin, A. David, J.F. Hervagault and J.L. Romette, *Proc. Natl. Acad. Sci. U.S.A.* 74 (1977) 5314.
- 5 S. Hardt, A. Naparstek, L.A. Segel and S.R. Caplan, in: *Analysis and control of immobilized enzyme systems*, eds. D. Thomas and J.P. Kernevez (North-Holland, Amsterdam, 1977) p. 9.
- 6 R. Blumenthal, S.R. Caplan and O. Kedem, *Biophys. J.* 7 (1967) 737.
- 7 A. Friboulet and D. Thomas, *Biophys. Chem.* 16 (1982) 139.
- 8 T. Teorell, *Prog. Biophys. Biophys. Chem.* 3 (1953) 305.
- 9 Y. Oren and A. Litan, *J. Phys. Chem.* 78 (1974) 1805.
- 10 T.R. Brumleve and R.P. Buck, *J. Electroanal. Chem.* 90 (1978) 1.
- 11 V.M. Aguilera, J. Garrido, S. Mafe and J. Pellicier, *J. Membrane Sci.* 28 (1986) 139.
- 12 D. Thomas and G. Broun, *Methods Enzymol.* 44 (1974) 901.
- 13 J. Henri and B. Louro, *C.R. Acad. Sci., Ser. I, Paris* 301 (1985) 763.
- 14 V. Ascher, J. Christiansen and R.D. Russel, *ACM Trans. Math. Software* 7 (1981) 209.
- 15 H. Oshima and S. Ohki, *Biophys. J.* 47 (1985) 673.